Defect and Diffusion Forum
ISSN: 1662-9507, Vol. 435, pp 141-150
doi:10.4028/p-Y3Lvjr

Submitted: 2023-12-13
Accepted: 2024-03-28
Online: 2024-09-19

Comprehensive Measurement and Simulation of Prototype Injection Moulds

Szabolcs Krizsma[1,a] and András Suplicz[1,2,b*]

[1]Department of Polymer Engineering, Faculty of Mechanical Engineering, Budapest University of Technology and Economics, Műegyetem rkp. 3., H-1111 Budapest, Hungary

[2]MTA-BME Lendület Lightweight Polymer Composites Research Group, Műegyetem rkp. 3., H- 1111 Budapest, Hungary

[a]krizsmasz@pt.bme.hu, [b]suplicz@pt.bme.hu

Keywords: Rapid tooling, state monitoring, injection moulding, simulation, finite element modeling

Abstract. The injection moulding industry is dynamically developing. The growing demand for more customizable products can be served by low or middle volume production using prototype moulds and inserts. The conventional material of prototype moulds is aluminum because of its excellent machinability, acceptable strength and stiffness and outstanding thermal conductivity. Prototype moulds are gaining ground in the injection moulding industry, yet their operational behavior (including exact mechanical and thermal process parameters) is largely unknown. We created a comprehensive state monitoring system that measures the operational strain, cavity pressure and temperature of different prototype injection moulds. This way, all important process parameters can be measured and the relations between the moulding parameters and the operational pressure loads, deformations and temperatures can be quantified and analysed.

Introduction

Injection moulding is the most versatile and significant polymer processing technology. The conventional application of injection moulding is the large volume production of parts because that is the economically feasible approach. However, the ever rising demand for mass customization brings new requirements and challenges for injection moulding. Mould makers turn to prototype injection moulds and interchangeable mould inserts, to make geometrically more diverse products in lower batches. The traditional material of prototype mould making is aluminum because of its excellent machinability, acceptable strength, stiffness and outstanding thermal conductivity. Kim et al [1] compared an injection mould insert made from high-strength aluminum alloy with an insert made from conventional tool steel. They found that the application of aluminum alloy reduces both the maximal surface temperature and the temperature amplitude of the moulds during operation. This way, the cyclic thermal load on the mould can be decreased. Kuo et al [2] compared a tool steel mould insert with an aluminum-filled epoxy resin insert based on their service life, and the surface roughness and dimensional stability of the injection moulded products. They found that the surface roughness of the injection moulded products were comparable for the two inserts below 1300 cycles. However, as the cycle number increased, the surface roughness of the parts made by the Al-filled epoxy resin insert exceeded that of the parts made by the tool steel insert. Kuo et al [3, 4] manufactured injection moulds using aluminum-filled epoxy resin. They were able to produce conformal cooling channels using wax patterns. By the combination of Al-filled epoxy resin tooling and wax patterns, they were able to produce large injection moulds cost-effectively.

Comprehensive metrology of injection moulds is rare to find as mould makers typically optimize their designs in a trial-and-error way through physical testing. Metrology is typically limited solely to cavity pressure measurement that can be a suitable product quality monitoring tool as it was proven by Struchtrup et al [5]. State-of-the-art mathematical methods like machine learning or neural networks can be applied effectively to monitor or predict key product quality indicators like mass and thickness based on the measured cavity pressure curves [6, 7]. Product quality monitoring is typically

focused on cavity pressure measurement, only a handful of studies recommend other measured quantities. Chen et al [8] suggest using the strain measurement of the injection moulding machine tie bar, while Su et al [9] propose the combined use of tie bar elongation measurement and nozzle pressure measurement to monitor product quality. Comprehensive sensoring and monitoring of injection moulds incorporates the simultaneous measurement of operational strains, cavity pressure and temperature [10, 11]. Such measurement system is especially useful when the injection moulding parameters have to be set optimally to increase mould life expectancy. Simultaneous measurement of strain, pressure and temperature also allows the analysis of correlations between them, which is extremely useful because the operational behavior can be understood in-depth.

Finite element modeling of injection moulds is also rare to find. Some research are available on their thermal simulation. Kovács et al [12] analysed the thermal state of polymeric mould inserts and applied injection moulding simulation to reproduce the measured temperature-time curves. They identified the specific heat, the thermal conductivity and the heat transfer coefficients as the major thermal parameters influencing the simulated temperature results. Zink et al [13] applied injection moulding simulation to model the operational temperature distribution of metallic mould inserts with different cooling channel layouts. They proved that the thermal simulation in the injection moulding simulation software could yield good temperature results.

This research article aims to fill knowledge gaps in the field of metrology of injection moulds as well as presenting a coupled simulation method to model the operational behavior of mould components under combined transient pressure and temperature load. The measurement method presented in this paper is applicable to gather strain, cavity pressure and temperature data and to validate the results of the coupled injection moulding simulation – finite element mechanical simulations. The presented simulation method can be applied if it is supported by an adequate amount of measurement and continuous validation of the simulated results.

Materials and Methods

We used a two-cavity mould housing for the injection mouldings and only the upper cavity was fit with the cavity insert. The lower cavity was shut off by a cylindrical runner insert. Strain was measured at two locations and a thermocouple measured the volumetric temperature of the aluminum mould insert. The measurement assembly is presented in Fig. 1.

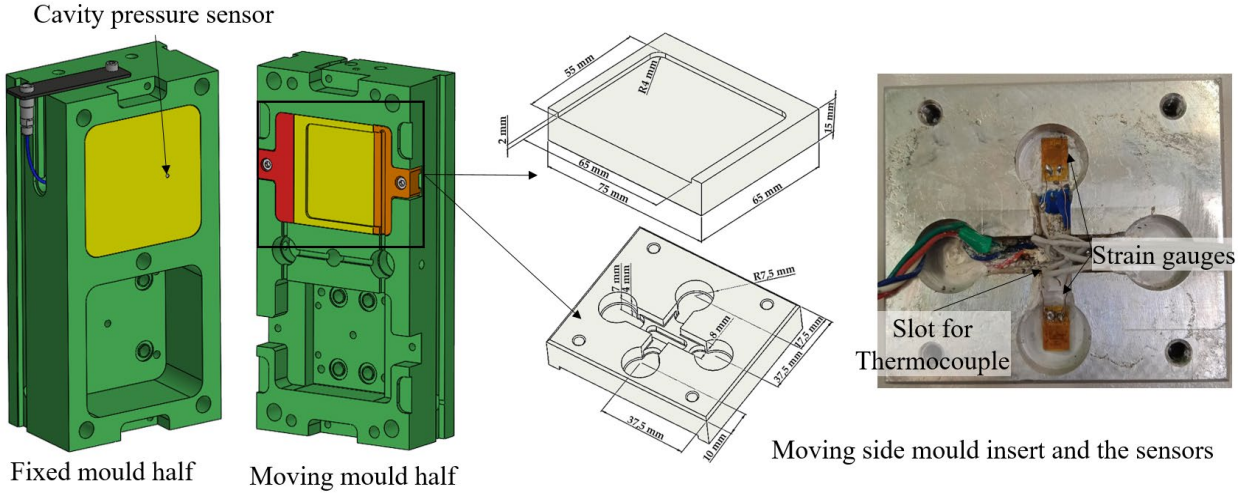

Fig. 1. The measurement assembly.

The cavity inserts and the washers underneath them were machined from EN AW 5754 O/H111. The relevant material properties are listed in Table 1. It is and excellent material grade for prototype moulds because of the combination of good mechanical properties, outstanding thermal conductivity and relatively easy machinability.

Table 1. Mechanical and thermal properties of EN AW 5754 O/H111.

Property (Unit)	Value
Tensile strength (MPa)	160–200
Elongation at break (%)	12
Modulus of elasticity (GPa)	68
Thermal conductivity (W/(m·K))	147
Coefficient of thermal expansion (1/K)	$24 \cdot 10^{-6}$
Specific heat (J/(kg·K))	900
Density (kg/m^3)	2.67

The injection moulded material was Tipplen H145F polypropylene homopolymer, manufactured by MOL Group Public Limited Company. It has a high melt flow rate (29 g/10 min at 230 °C and 2.16 kg load) and low processing temperature range (190-230 °C). We injection moulded using an Arburg Allrounder Advance 270S 400-170 injection moulding machine (screw diameter: 30 mm). The injection moulding parameters are presented in Table 2. It can be seen that a low melt temperature was applied. Injection speed was set so that the filling time of the plate was approximately 1 second. A low clamping force was sufficient due to the relatively small dimensions of the injection moulded plate (65 x 55 x 2 mm) and the low required injection pressure. Long idle times were kept between the cycles because no active mould cooling was applied. We started with 10 cycles injection moulded at 75 bar constant holding pressure, and then we increased the holding pressure from 50 bar to 300 bar using 25 bar steps in every second cycle.

Table 2. The injection moulding parameters.

Parameter (Unit)	Value
Melt temperature (°C)	190
Injection speed (cm^3/s)	15
Injection pressure limit (bar)	500
Clamping force (t)	5
Dose volume (cm^3)	40
Switchover point (cm^3)	25.5
Holding pressure (bar)	50 to 300
Holding time (s)	15
Residual cooling time (s)	30
Idle time (s)	250

Results and Discussions

We started injection moulding with 75 bar constant holding pressure and we injection moulded 10 cycles at that level. The measured operational strains and cavity pressure curves are presented in Fig. 2. It can be seen that a sharp increase occurs both in the strains and the cavity pressure during the filling phase as the melt is injected into the cavity at high speed. As the complete volumetric filling is done and the melt hits the cavity wall at the end of the flow length, the increase in strain becomes slower at the near gate location and even a decrease can be observed at the far from the gate location as the transient pressure load of the melt decreases temporarily after volumetric filling. A drop can be observed on the cavity pressure curve right after the switchover point because the injection

pressure decreases from the maximal filling pressure of approximately 320 bar to the pre-set 75 bar. After the fluctuation caused by this pressure drop, the cavity pressure increases again as the product is compressed by the additional injected melt of the holding phase to compensate the shrinkage. The increase in the cavity pressure happens until gate freeze. After that, no additional material can be injected and the cavity pressure stabilizes at approximately 15 bar for the rest of the injection moulding cycle. The strain near the gate reaches its maximum of approximately 0.018% at around gate freeze and begins its relatively slow decrease in the second part of the holding and later in the residual cooling phase. It is because the injected melt solidifies and the product cools down and shrinks. The product gradually detaches from the cavity wall, unloading the mould insert. A stepwise drop can be seen in the operational strain at the end of the cycle as the clamping force is removed and the mold is opened. After part ejection, the thermal strain of the mould insert decreases as the insert itself cools down to the temperature before the cycle.

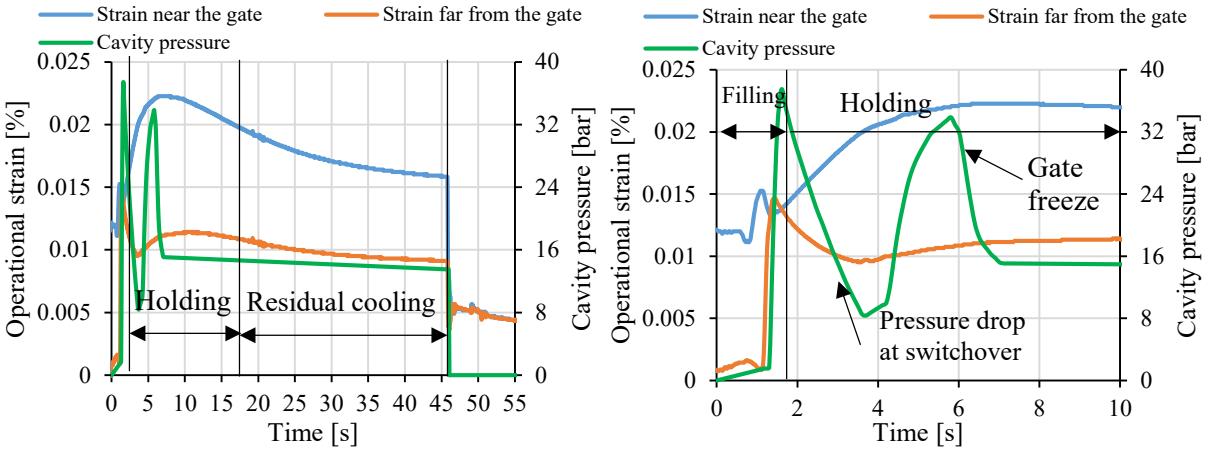

Fig. 2. The measured operational strains and cavity pressure at 75 bar holding pressure.

After the 10 cycles injection moulded at 75 bars we increased the holding pressure. The strain and cavity pressure results of the cycles injection moulded at 150 bar holding pressure are presented in Fig. 3. Similarities can be observed with the strain results of Fig. 2. The strain near the gate remained nearly identical with the strain measured at 75 bar holding pressure, while the strain far from the gate grew from 0.015% to 0.021%. The maximal cavity pressure (measured far from the gate) at switchover also grew from 36 bar to 64 bar which explains the growth in the strain far from the gate. Following the switchover, the pressure also drops to approximately 8 bars which is quite similar to the minimal pressure measured at 75 bar holding pressure. Following the pressure drop and the application of the 150 bar holding pressure, the cavity pressure grows again until gate freeze, at 10 seconds. Following gate freeze, the pressure stabilizes at 40 bar, which is higher than the 15 bar cavity pressure measured at 75 bar holding pressure.

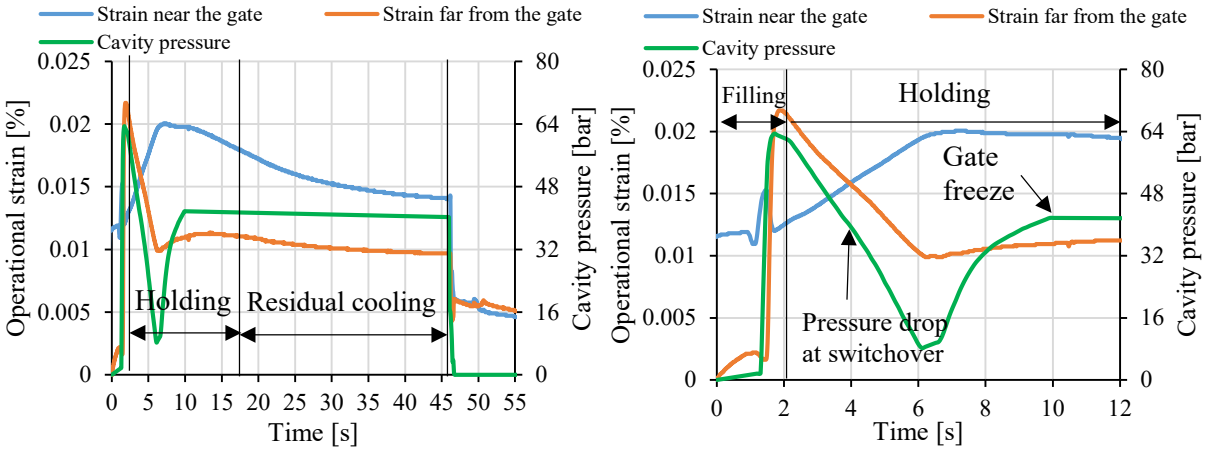

Fig.3. The measured operational strains and cavity pressure at 150 bar holding pressure.

Maximal operational strains were correlated with the corresponding maximal cavity pressures and the results are shown in Fig. 4. A satisfactory linear relation (R^2=0.906) was found between the maximal cavity pressure and the maximal operational strain which can be contributed to the linear elastic behavior of the aluminum mould material. This strong relation is an indication that strain measurement and cavity pressure measurement can be interchangeable.

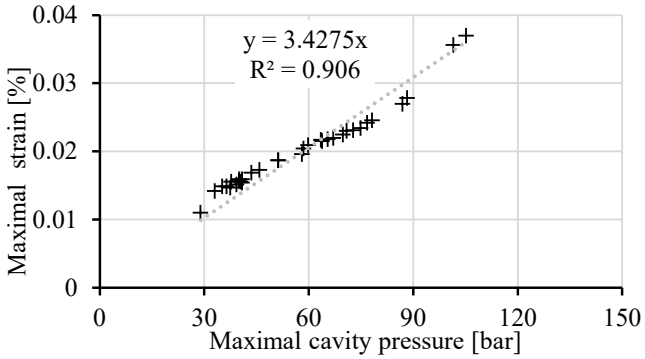

Fig. 4. Correlational diagram between maximal cavity pressure and maximal operational strain.

Modeling the operational state of the mould insert

We set up a combined injection moulding simulation – finite element mechanical simulation to model the operational state of the mould insert. It consists of the following steps. First, the mould was meshed in Autodesk Moldflow Insight 2021, where a Fill + Pack analysis was run and the time dependent pressure and temperature load together with the mould mesh was exported using the "mpi2ans" macro. Following that, the mould mesh was imported into ANSYS Workbench Mechanical 2019 and a transient thermal simulation was set up. This model was built to reproduce the thermal state of the mould during operation. After successfully modeling the temperature of the mould insert (measured by the thermocouple) the transient temperature field was coupled with a structural mechanical simulation, where the mould insert's deformations are modeled and compared with the measured strains.

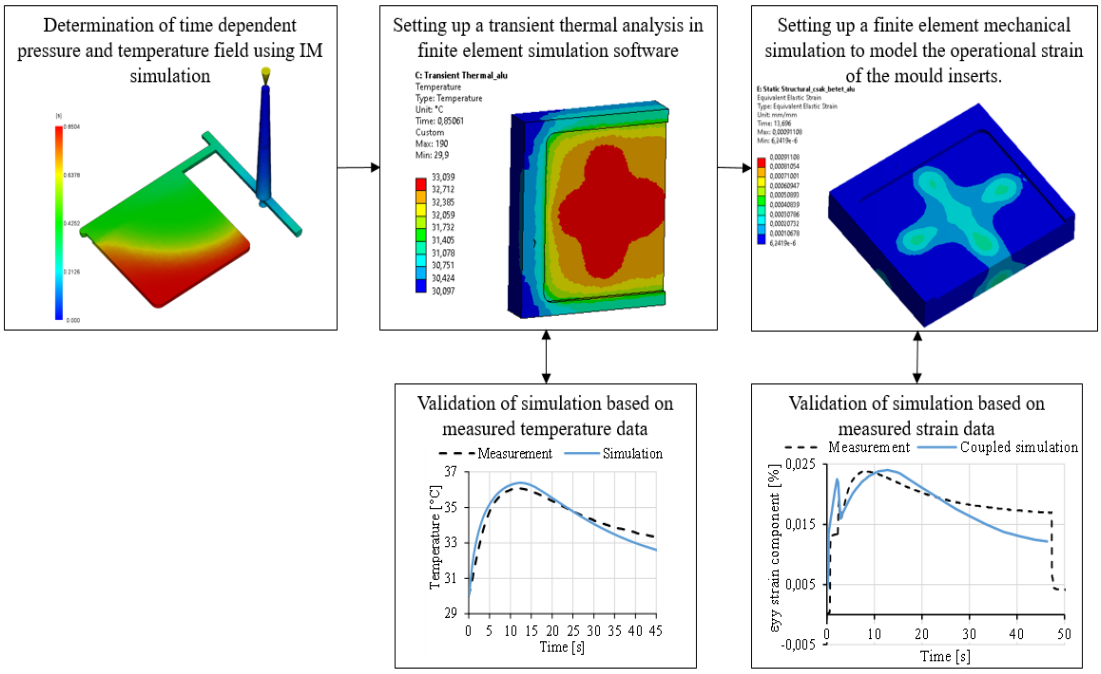

Fig. 5. Flowchart of the coupled injection moulding simulation – finite element mechanical simulation.

Fig.6 shows the fill pattern of the injection moulded product determined by the Moldflow simulation. The fill pattern shows excellent correspondence with the actual short-shot products proving the adequacy of the injection moulding simulation. The fill time also shows good agreement with the injection moulding experiments.

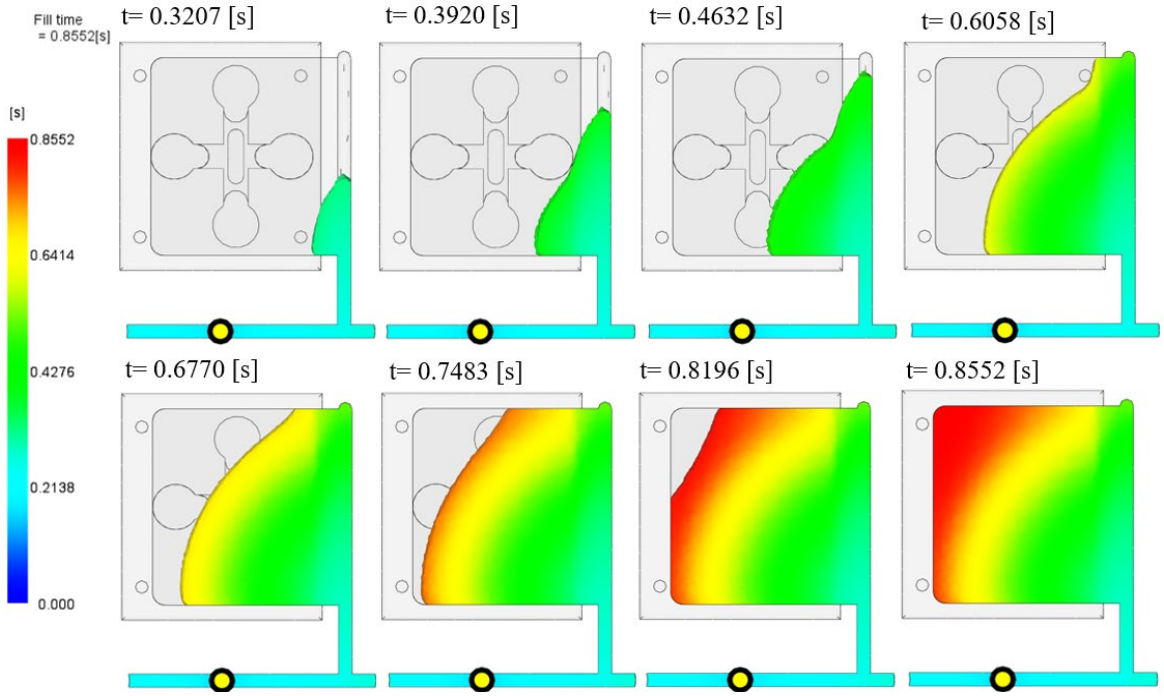

Fig.6. Fill pattern of the cavity calculated by injection moulding simulation.

The transient temperature field of the injection mould insert is presented at some characteristic time points in Fig.7. The heating of the insert is very fast due to the outstanding thermal conductivity of the aluminum mould material. Maximal insert temperature of 36 °C is already reached at approximately 12.5 seconds from the start of the cycle and basically the entire cross section of the mould insert is heated up. At the end of the cycle (at 45.8 seconds) the mould insert cools back to 32-33 °C which is a small increment compared to the 30 °C at the start of the cycle.

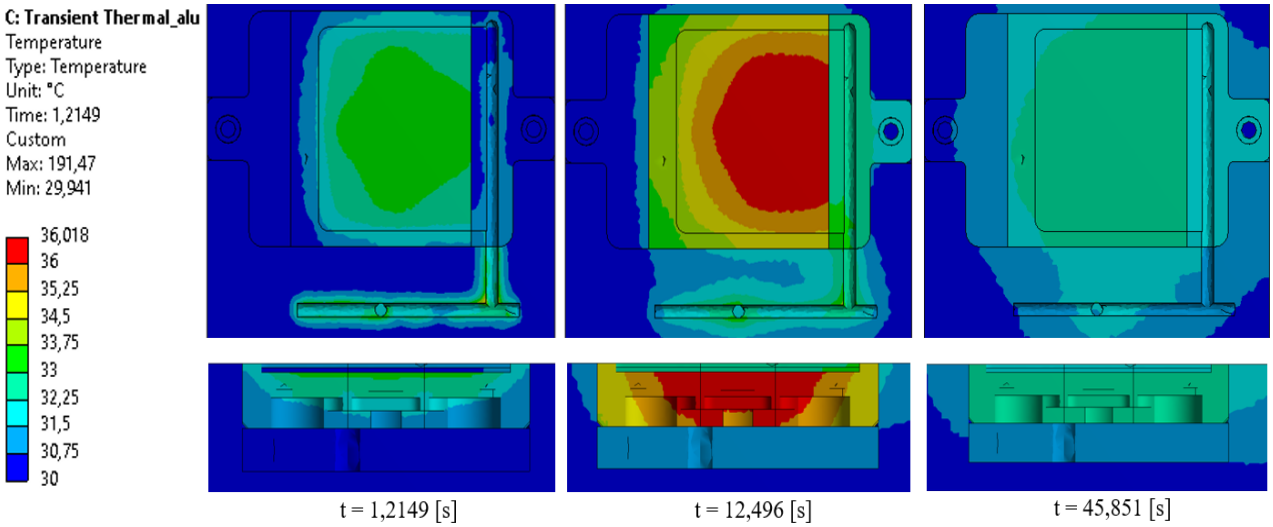

Fig.7. Calculated temperature distribution of the aluminum mould insert during the injection moulding cycle.

The results were validated by the thermocouple temperature measurement (already presented in Fig.1). A very good agreement can be found between the measured temperature – time curve and the simulation result. As it was already discussed, the heating of the insert is fast and maximal insert temperature is already reached at 12.5 seconds from the start of the cycle. After that, the insert cools down at a slower pace and the insert temperature reaches approximately 33 °C by the time of part ejection. Temperature measurement is a key element to validate the finite element simulation results.

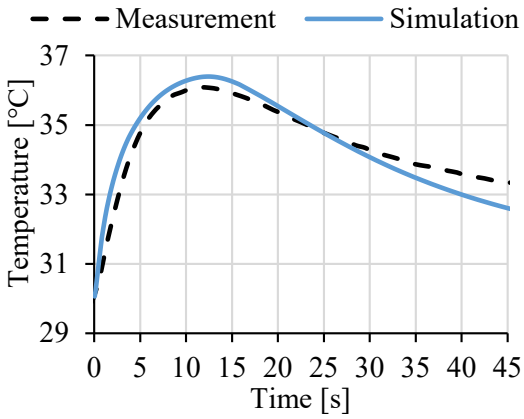

Fig.8. Comparison of the calculated temperature time-curve at the location of the thermocouple and the measured temperature-time curve.

A mechanical simulation was set up following the proper modeling of the temperature field of the mould insert. The mould insert was isolated and a single-body mechanical model was created for the insert in order to reduce the required computation effort. The surfaces had boundary conditions applied where the insert touches other mould components. These so-called “Compression only supports” simulate contact with a perfectly rigid wall. The mould insert cannot cross these surfaces but it can detach from them. Operational deformation of the mould insert has two fundamental sources: the first is the pressure load acting on the cavity surfaces, the second is the thermal expansion caused by the heat load of the injected melt. The time dependent pressure load was imported from Moldflow and it was applied on the mould insert in the mechanical simulation. The time dependent temperature load was already calculated by the preceding thermal simulation. The equivalent elastic strain result of the mould insert was also analysed and it is presented in Fig.9. It can be seen that strain is primarily localized around the area of the slots for the strain gauges.

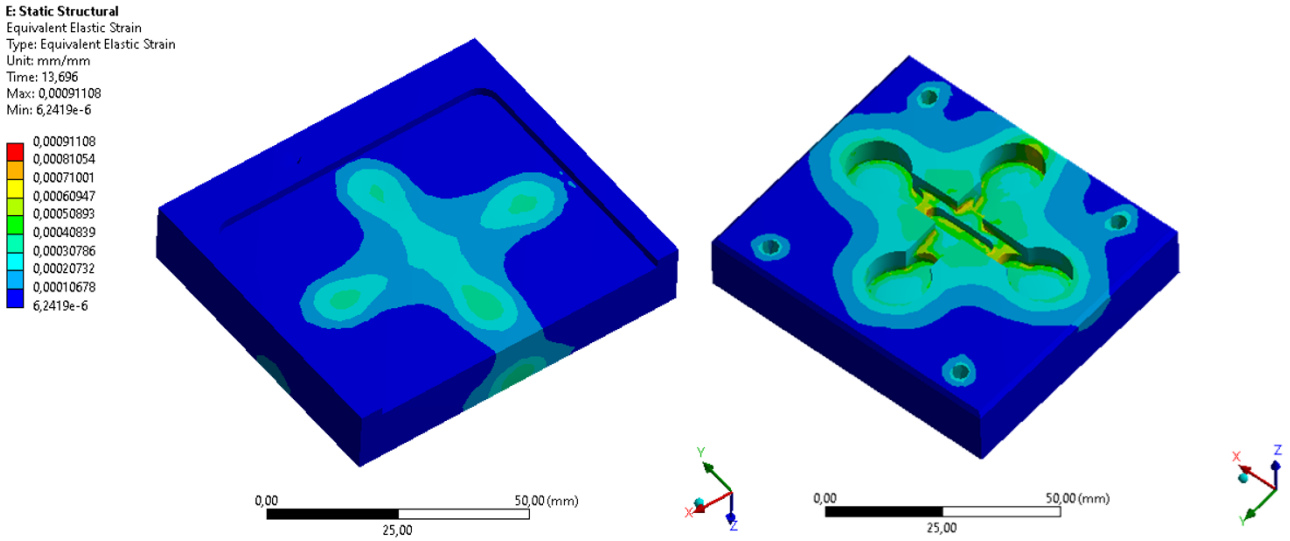

Fig.9. Calculated equivalent elastic strain distribution of the mould insert at the end of the holding phase.

The calculated Y directional normal strain was compared to the measured strain curves as it is presented in Fig.10. A nice agreement was found between the measurement and the simulation that proves the accuracy and adequacy of the presented simulation method. Maximal operational strain was modeled with accuracy and the time dependent characteristic of the operational strain was also captured. The simulation also captures the main segments of the injection moulding cycle as it is shown in Fig.10. The minor deviations between the measurement and the simulation can be traced back to the imperfect contacts between the mould components that are neglected by the simulation. Operational strain measurement is necessary for the proper validation of the finite element mechanical simulation models.

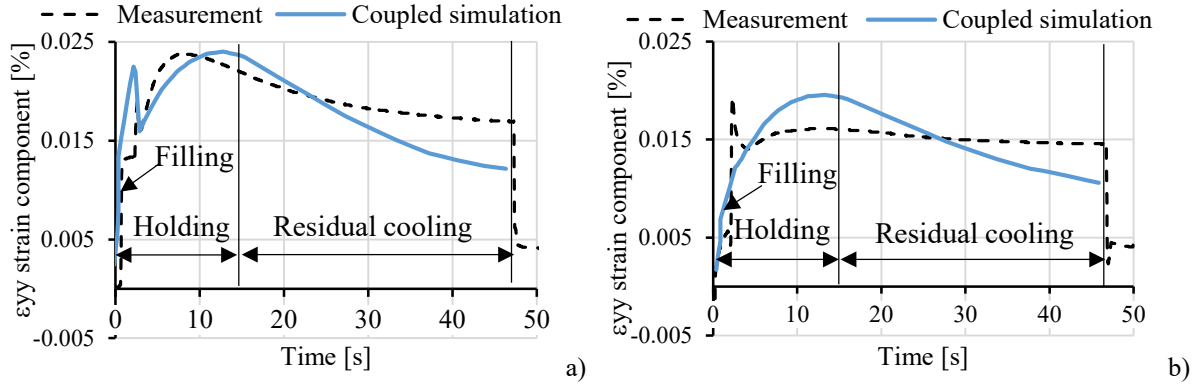

Fig.10. Comparison of the calculated and the measured ε_{yy} normal strain time-curve at the location of the near the gate a) and far from the gate b) strain gauges.

Summary

In this paper, a comprehensive state monitoring system was presented for injection mould inserts. This measurement system consists of the simultaneous measurement of strains, cavity pressure and temperature. This way, a broad view can be obtained about the behavior of the injection mould inserts and the effect of the varying injection moulding parameters can be quantified on their mechanical and thermal state. We presented the operational strain and cavity pressure curves at two different holding pressures (75 bar and 150 bar) and highlighted the main injection moulding cycle elements on these curves. We also gave an in-depth explanation of the main cycle elements that determine the shape of the strain and cavity pressure curves. We also analysed the correlations between the maximal operational strains and maximal cavity pressures and found a strong linear relation between them (R^2=0.906). This strong linear relation indicates that there is a confident correspondence between the results of the strain measurement and the cavity pressure measurement.

Following the presentation of the measured results, a novel simulation approach was outlined. It comprises of a coupled injection moulding simulation – finite element mechanical modelling approach. Meshing of the mould components is carried out in Autodesk Moldflow Insight followed by an injection moulding simulation to determine the time-dependent pressure and temperature fields. After that, the simulation results are exported to ANSYS Workbench where a transient thermal simulation is made. This thermal simulation is necessary to calculate the time dependent temperature field in not just the product but in the surrounding mould components as well. Operational temperature measurement is vital for the validation of the simulation results. After the thermal simulation, the calculated transient temperature field is exported to a mechanical simulation. Mechanical simulation also requires the time dependent pressure load, calculated prior by the injection moulding simulation. The combination of the thermal and the mechanical load can be applied on the analysed mould component and the calculated mould deformations then have to be validated. Operational strain measurement is an ideal tool to validate the mechanical simulation results.

Acknowledgements

Supported by the ÚNKP-23-3-II-BME-31 New National Excellence Program of the Ministry for Culture and Innovation from the source of the National Research, Development and Innovation Fund. Project no. RRF-2.3.1-21-2022-00009, titled National Laboratory for Renewable Energy has been implemented with the support provided by the Recovery and Resilience Facility of the European Union within the framework of Programme Széchenyi Plan Plus. This work was supported by the National Research, Development and Innovation Office, Hungary (OTKA FK138501).

References

[1] J. Kim., R. Smierciak, Y.S. Shin, L. Cooper, Advances in Aluminum Mold Block for Plastic Injection Molding Operations. In: Weiland, H., Rollett, A.D., Cassada, W.A. (eds) ICAA13 Pittsburgh (2012). https://doi.org/10.1007/978-3-319-48761-8_243

[2] C.-C. Kuo, X.-Y Pan, Development of a Rapid Tool for Metal Injection Molding Using Aluminum-Filled Epoxy Resins. Polymers 15 (2023) 3513. https://doi.org/10.3390/polym15173513

[3] C.-C. Kuo, Y. J. Zhu, Y. Z. Wu, Development and application of a large injection mold with conformal cooling channels. Int J Adv Manuf Technol 103 (2019) 689–701. https://doi.org/10.1007/s00170-019-03614-4

[4] C.-C. Kuo, T.-D. Nguyen, Y.-J. Zhu, S.-X. Lin, Rapid Development of an Injection Mold with High Cooling Performance Using Molding Simulation and Rapid Tooling Technology. Micromachine 12 (2021) 311. https://doi.org/10.3390/mi12030311

[5] A. S. Struchtrup, D. Kvaktun, R. Schiffers, A holistic approach to part quality prediction in injection molding based on machine learning Advances in Polymer Processing 2020, Springer, Berlin/Heidelberg, Germany (2020) 137-149, https://doi.org/10.1007/978-3-662-60809-8_12

[6] R. D. Párizs, D. Török, T. Ageyeva, J. G. Kovács, Machine Learning in Injection Molding: An Industry 4.0 Method of Quality Prediction, Sensors, 22, (2022) 2704/1-2704/16. https://doi.org/10.3390/s22072704

[7] K.-C. Ke, M.-S. Huang, Quality classification of injection-molded components by using quality indices, grading, and machine learning, Polymers, 13(3), (2021) 353. https://doi.org/10.3390/polym13030353

[8] J.-Y. Chen, J.-X. Zhuang, M.-S. Huang, Enhancing the quality stability of injection molded parts by adjusting V/P switchover point and holding pressure, Polymer, 213, (2021) 123332. https://doi.org/10.1016/j.polymer.2020.123332

[9] C.-W. Su, W.-J. Su, F.-J. Cheng, G.-Y. Liou, S.-J. Hwang, H.-S. Peng, H.-Y. Chu, Optimization process parameters and adaptive quality monitoring injection molding process for materials with different viscosity, Polymer Testing, 109, (2022) 107526. https://doi.org/10.1016/j.polymertesting.2022.107526

[10] Sz. Krizsma, A Suplicz, Comprehensive in-mould state monitoring of Material Jetting additively manufactured and machined aluminium injection moulds, Journal of Manufacturing Processes, 84, pp 1298-1309, 2022. https://doi.org/10.1016/j.jmapro.2022.10.070

[11] Sz. G. Krizsma, N. K. Kovács, J. G. Kovács, A. Suplicz, In-situ monitoring of deformation in rapid prototyped injection molds, Additive Manufacturing, 42, (2021) 102001/1-102001/8. https://doi.org/10.1016/j.addma.2021.102001

[12] J.G. Kovács, F. Szabó, N.K. Kovács, A. Suplicz, B. Zink, T. Tábi, H. Hargitai, Thermal simulations and measurements for rapid tool inserts in injection molding applications, Applied Thermal Engineering, 85(25), (2015) pp. 44-51 https://doi.org/10.1016/j.applthermaleng. 2015.03.075

[13] B. Zink, F. Szabó, I. Hatos, A. Suplicz, N. K. Kovács, H. Hargitai, T. Tábi, J. G. Kovács, Enhanced Injection Molding Simulation of Advanced Injection Molds. Polymers, 9 (2017) 77. https://doi.org/10.3390/polym9020077